Draft version January 7, 2021
Preprint typeset using LaTeX style emulateapj v. 08/13/06

INNER AND OUTER ORBITS IN 13 RESOLVED HIERARCHICAL STELLAR SYSTEMS

A. Tokovinin
Cerro Tololo Inter-American Observatory — NSF's NOIRLab, Casilla 603, La Serena, Chile
Draft version January 7, 2021

ABSTRACT

Orbits of inner and outer subsystems in 13 triple or higher-order stellar systems are computed or updated using position measurements and, in three cases, radial velocities. The goal is to determine mutual orbital inclinations, period ratios, and masses to complement the statistics of hierarchical systems. Effect of the subsystems on the motion in the outer orbits (wobble) is explicitly modeled to determine inner mass ratios. Stars studied here (HD 5408, 8036, 9770, 15089, 29310, 286955, 29316, 140538, 144362, 154621, 156034, 185655, and 213235) are bright and nearby (from 15 pc to 150 pc). Their inner periods range from 1.7 yr to 49 yr, and the outer periods from 83 to 2400 yr. Some long-period outer orbits are poorly constrained. Four astrometric inner orbits and one outer orbit are computed for the first time.

Subject headings: binaries:visual; binaries:general

1. INTRODUCTION

Architecture of hierarchical stellar systems is interesting for several reasons. Period ratios, mutual orbit orientation, and distribution of masses are related to the processes of formation and early dynamical evolution of these systems, and therefore inform us on the star formation in general. Most stars are born in groups, hence properties of binary and higher-order systems are very relevant. Life and death of stars is also affected by their companions in various ways. Close pairs can form within hierarchical systems by their dynamical evolution on a long (compared to the formation) time scale. Late mergers or collisions can create unusual objects. Hamers (2020) explored outcomes of dynamical evolution using data on real hierarchical systems collected in the Multiple Star Catalog (MSC, Tokovinin 2018a).

This study is aimed at calculation or improvement of visual or astrometric orbits of the inner and outer subsystems belonging to the same hierarchy. There are only a few dozen systems where this is possible; the list of 54 such objects with outer periods less than 1000 yr is given in Tokovinin (2017b). On the one hand, most outer systems with their typically long periods lack adequate coverage needed for orbit calculation. On the other hand, resolution of inner subsystems is possible when they are relatively close to the Sun and their periods are not too short. Combination of both constraints results in a sample of hierarchical systems with comparable periods and separations and, typically, with similar masses. Obviously, the observed sample is not representative of hierarchical systems in the statistical sense. However, hierarchies with comparable periods are most interesting from the dynamical perspective because interactions between their subsystems might be important.

The observed motions in a hierarchical system are modeled here by two Keplerian orbits. In reality dynamical interactions cause evolution of those orbits over time. These effects are too small to be detected in our systems. Given the orbital elements and the estimated masses, the long-term dynamical evolution can be explored numerically (e.g. Xia & Fu 2015; Hamers 2020), but this is outside the scope of the present study.

Table 1 presents the 13 hierarchies studied here. Its first three columns identify the systems by the Washington Double Star (WDS, Mason et al. 2001) codes based on J2000 positions, HD, and HIP numbers. The combined visual magnitudes come from Simbad, the parallaxes are either measured by Gaia (Gaia collaboration 2018) or estimated from the masses and orbits as explained below. Types of the orbits (visual, astrometric, or spectroscopic) and periods of the outer and inner subsystems are given. Astrometric or visual orbits computed for the first time here are marked by asterisks. Some of these hierarchies have more than three components, but they are effectively treated here as triples. Components' masses of these triples and the total number of components are given in the last two columns (inner subsystem in brackets).

Most of these bright and nearby hierarchies had previous determinations of their inner and outer visual orbits or even a joint analysis (e.g. Heintz 1996), so why a new study is needed? First, outer and inner orbits are fitted here jointly, including the wobble caused by the subsystem. Second, recent speckle data are used and appropriate weights are applied; radial velocities (RVs) are included when available to improve the accuracy. Masses of the components are estimated using new Gaia parallaxes and absolute magnitudes (or isochrones for evolved stars). Consistency between parallaxes, orbits, and estimated mass sums is achieved; elements of poorly constrained long-period orbits are chosen to match the mass sums. Finally, accuracy of the orbital elements is evaluated, as well as the reliability of mutual inclination and period ratios computed from these orbits. Two astrometric inner orbits of spectroscopic subsystems, two visual inner orbits, and one outer orbit are first-time solutions. This study continues previous work on the orbits of hierarchical systems (Tokovinin & Latham 2017, 2020; Tokovinin 2018b).

Components of multiple systems are designated by sequences of letters and numbers, as in the WDS. Subsystems are denoted as two components joined by a comma.

Electronic address: atokovinin@ctio.noao.edu

TABLE 1
List of multiple systems

WDS (J2000)	HD	HIP	V (mag)	ϖ^a (mas)	Outer[b]	P_{out} (yr)	Inner[b]	P_{in} (yr)	Masses ($\mathcal{M}_\odot$)	N_{comp}
00568+6022	5408	4440	5.55	5.6 D	V	84.1	V,A,S1	4.9	(3.4+4.1)+3.4	4
01198−0031	8036	6226	5.87	7.76 G	V	1000:	V,A	27.1	2.5+(2.1+1.8)	3
01350−2955	9770	7372	7.08	45.83 G	V	121	V,A	4.56	(0.9+1.5)+0.6	4
02291+6724	15089	11569	4.52	22.22 G	V	2400:	V,A	48.7	(2.1+0.9)+1.3	5
04375+1509	29310	21543	7.54	20.69 G	V,S1	125	S1,A*	2.0	(1.1+0.3)+0.7	3
04397+0952	286955	21710	9.19	34.04 G	V,S1	285	S1,A*	1.7	(0.75+0.15)+0.5	4
04400+5328	29316	21730	5.35	13.0 D	V	660:	V,A*	26.3	(1.9+1.5)+1.5	3
15440+0231	140538	77052	5.87	67.71 G	V	900:	V,A	6.6	1.0+(0.3+0.3)	3
16057−0617	144362	78849	6.36	12.03 G	V	300:	V,A	5.0	(1.6+1.6)+1.1	4
17066+0039	154621	83716	8.28	17.90 G	V	900:	V,A	6.3	1.0+(0.7+0.7)	3
17157−0949	156034	84430	6.98	7.9 D	V	137	V	5.3	1.7+(1.4+1.3)	3
19453−6823	185655	97196	10.06	21.0 G	V*	84	V,A	4.4	0.8+(0.5+0.4)	3
22300+0426	213235	111062	5.51	18.84 G	V	124	V,A*	2.1	1.7+(1.2+1.1)	3

[a]Parallax codes: G — Gaia (Gaia collaboration 2018), D — dynamical.
[b]System types: V — visual orbit, A — astrometric orbit, S1 — single-lined spectroscopic orbit, * — first orbit.

Thus, A,B means a subsystem with components A and B, while AB stands for the composite component (center of mass) in a wider pair AB,C. I try to avoid using the outdated discoverer codes given in the WDS, but mention them for completeness in the notes on individual systems.

Section 2 presents the methods briefly. The main part of the paper is Section 3, where each hierarchy is discussed individually, and masses and other parameters are estimated. A short summary in Section 4 closes the paper.

2. DATA AND METHODS

The orbit of a visual binary is defined by the seven Campbell elements $P, T, e, a, \Omega, \omega, i$ (in standard notation). Fitting these elements to position measurements $\theta(t)$ and $\rho(t)$ is a classical problem with many solutions given in the literature. I use the least-squares fit with weights inversely proportional to the square of measurement errors σ_i^2. However, the actual errors are not Gaussian and are not well known, leaving room for subjective choices; different orbits can be derived from the same data, depending on the method and weights.

The observed motion in a resolved triple system (e.g. Aa,Ab and A,B) is modeled here by two Keplerian orbits and the wobble factor f, hence there are 15 free parameters; more parameters (e.g. the inner and outer RV amplitudes K_1, K_3, and the system velocity γ) are fitted when the RV measurements are available. The angles Ω and ω are chosen to fit the RV of the primary component, otherwise both can be changed simultaneously by 180°. The wobble factor is the ratio of the wave amplitude in the outer orbit caused by the subsystem to the inner semimajor axis. When the outer positions of Aa,B refer to the resolved inner subsystem, $f = q/(1+q)$ is directly related to the inner mass ratio $q_{\rm Aa,Ab}$; it is also called the fractional mass (Heintz 1996; Tokovinin & Latham 2017). When the positions of the outer component B are measured relative to the photo-center of the unresolved inner subsystem, e.g. A,B, then the wobble factor $f^* = f - r/(1+r)$ depends on the light ratio $r = 10^{-0.4\Delta m}$. For example, if the inner subsystem consists of two identical stars, $f = 0.5$ and $f^* = 0$. When the inner subsystem is not resolved, I set its semimajor axis to the value calculated from the period and mass and fit the wobble factor to determine the axis of the astrometric orbit.

I use the IDL code `orbit3.pro`[1] to fit both orbits simultaneously (Tokovinin & Latham 2017; Tokovinin 2018b; Tokovinin & Latham 2020). Its modification `orbit4.pro` distinguishes between outer positions measured from a resolved and unresolved inner system; the factor f is fitted, while the ratio f^*/f is fixed to a value deduced from a model, e.g. zero for equal-mass subsystems. Often accurate speckle measurements refer to the resolved subsystem Aa,B, while the remaining unresolved micrometer measurements are so crude that the photocenter wobble is lost in their noise, making the distinction between f and f^* irrelevant.

The position measurements were retrieved from the WDS database (Mason et al. 2001) on my request and, where possible, complemented by the recent speckle interferometry at the Southern Astrophysical Research (SOAR) 4.1 m telescope (Tokovinin et al. 2020, and references therein). The latest SOAR observations are made in 2020.8. The SOAR measurements and the data from telescopes with apertures of 6 m and larger are assigned errors of 1–2 mas, speckle interferometry at other 4 m class telescopes is assumed to have errors of 5 mas. For smaller apertures, the errors are correspondingly larger. The visual micrometer measurements are assumed to have errors from 0.″05 to 0.″25, depending on the separation. These errors are poorly known, while the old data vary in quality, depending on the observer. I liberally deleted the largest historical outliers and downweighted some other micrometer measurements. The system of weights used here privileges the speckle data and is different from the weights adopted by the orbit catalog (Hartkopf et al. 2001). The existing outer orbits of triple systems were typically computed by simple Keplerian fits, neglecting the wobble; its explicit modeling here improves the accuracy.

Some long-period outer orbits considered here have only a short arc covered by the observations, resulting in the loosely constrained elements. Previously computed orbits of these pairs have grade 5 (preliminary) in the catalog (Hartkopf et al. 2001). While the standard approach uses only the position measurements, I consider here ad-

[1] Codebase: http://dx.doi.org/10.5281/zenodo.321854

ditional information on the mass sum, parallax, and, in some cases, the RVs. Large errors of some elements (e.g. period or inclination) in the initial, unconstrained, fit indicate that a wide range of orbits is compatible with the data. Poorly defined elements usually strongly correlate with other elements. I fix some poorly defined elements to satisfy the additional constraints on the mass sum and fit the remaining elements; the formal errors of the fitted elements in such orbits are in fact only lower limits. Even uncertain long-period orbits of hierarchical systems are useful because they accurately represent the observations, serve as a reference for measuring the wobble, and allow calculation of the mutual inclination Φ. In most cases, the true ascending nodes of the inner and/or outer orbits are not known, and two alternative values of Φ are possible (Tokovinin 2017b).

Masses of main-sequence stars are estimated from their absolute visual magnitudes using standard relations (Pecaut & Mamajek 2013). The parallaxes are measured by Gaia (Gaia collaboration 2018). However, its current data release does not account for the non-linear motion of binaries. Gaia parallaxes and proper motions (PMs) of binary stars may have large errors and biases, and the relation between these effects and the orbital parameters is complex (Penoyre et al. 2020). The short-term PM of binaries measured by Gaia often differs from their long-term PM deduced from the Hipparcos and Gaia positions. This PM anomaly (Brandt 2018) is a manifestation of astrometric acceleration; sometimes it helps to constrain or verify the orbits. I use the more accurate Gaia parallaxes of other (non-binary) components of multiple systems when they are available. Otherwise, dynamical parallaxes computed from the orbits and the estimated masses are currently the best distance measurements.

All orbit plots in the next section (e.g. Figure 1) are similar. They show the outer orbit, including the wobble, by the wavy line. Measurements of the outer pair (asterisks if resolved, squares and crosses otherwise) are connected to the expected positions on the orbit by short dotted lines. The scale is in arcseconds, the orientation is standard (north up, east left), and the primary component (large asterisk) is located at the coordinate origin. The orbit of the inner subsystem is plotted at the center, on the same scale, by the magenta dash ellipse and triangles. Even if the inner subsystem belongs to the secondary component, its orbit is plotted around the center; in this case, the wobble factor is negative. Each plot also contains a graph representing the hierarchical structure of the multiple system (the mobile diagram). Masses of stars and orbital periods in italics accompany these diagrams.

Elements of visual orbits (including the wobble factor) and their errors are listed in Table 2. The last column gives the RV amplitudes when the RVs were used; the systemic velocities are given in the discussion of individual systems. As only published RVs are used, they are not duplicated here. The position measurements, their adopted errors, and residuals to the orbits are assembled in Table 3, published in full electronically.

3. INDIVIDUAL SYSTEMS

3.1. *00568+6022 (ADS 784, HR 266)*

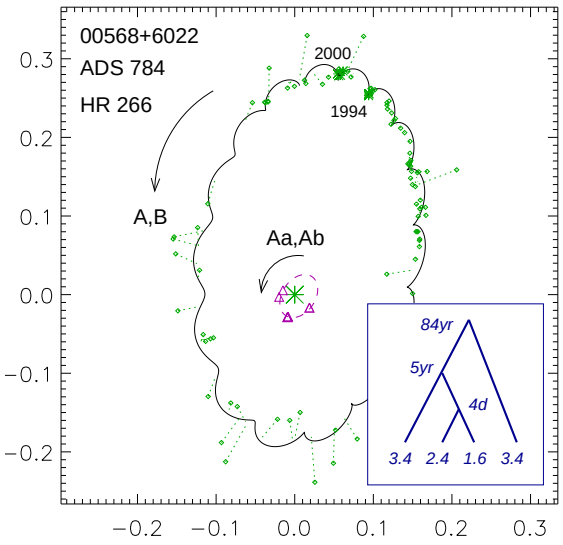

FIG. 1.— Outer and intermediate orbits of ADS 784 (periods 84 yr and 5 yr). In this and following figures, the wavy line marks the outer orbit. Measured positions (asterisks and crosses) are connected to the expected positions by short dotted lines. Scale in arcseconds, north up, east left, primary component at coordinate origin. The inner orbit is plotted at the center on the same scale (magenta ellipse and triangles). The blue graph shows the hierarchical structure of the complete system, with approximate periods and masses in italics.

HR 266 (ADS 784) is an early-type quadruple system. The outer pair is a 84 yr visual binary BU 1099. Its orbit, fully covered and quite accurate, is only slightly updated here. Cole et a. (1992) published a detailed study of this system, including spectroscopic orbits of the inner 4.2 day double-lined spectroscopic binary and its 5 yr orbit in an intermediate subsystem, which was also discovered independently by the wavy motion of A,B. Therefore, this is a 3+1 hierarchy where a close binary has a tertiary companion and this triple is orbited by another, more distant visual companion (Figure 1).

Schoeller et al. (1998) reported direct resolution of the intermediate pair Aa,Ab at 25 mas separation, near the diffraction limit of the 6 m telescope. While Cole et al. attributed the spectroscopic triple to the secondary visual component B, in fact the component A has been resolved. Balega et al. (1999) revise the system model where the inner triple belongs to the component A and show that it does not contradict the spectroscopy of Cole et al. However, their model identifies the inner spectroscopic binary with Aa and predicts zero wobble in the unresolved measurements of A,B because the mass and light ratios of the 5 yr subsystem are nearly equal (about 0.5), canceling the photo-center wobble. I repeated their analysis and reached the same conclusion that contradicts the observed wavy motion of A,B. Docobo & Andrade (2006) computed a crude visual orbit of the 5 yr pair (without using the RVs) and also estimated masses from the absolute magnitudes. They found that most of the mass is concentrated in the inner triple, but still call this component B.

Here I attempt to clarify the confusion regarding this system by attributing the inner 4-day pair to the secondary component Ab and denoting it as Ab1,Ab2. Speckle observations published since the last analysis by Balega et al. and the RVs of the center-of-mass of Ab

TABLE 2
Orbital Elements

WDS	System	P (yr)	T (yr)	e	a ($''$)	Ω (deg)	ω (deg)	i (deg)	f	K (km s^{-1})
00568+6022	Aab,Ac	4.899	2003.565	0.260	0.0309	146.8	279.2	47.3	0.346	11.18
		±0.009	±0.038	±0.017	±0.0012	±2.5	±2.9	±3.2	±0.065	±0.24
00568+6022	A,B	84.10	1953.59	0.225	0.237	171.5	343.5	53.6	...	4.30
		±0.84	±0.83	±0.010	±0.006	±0.9	±3.6	±0.9	...	fixed
01198−0031	B,C	27.13	1994.92	0.205	0.1108	41.2	343.2	18.5	−0.466	...
		±0.08	±0.19	±0.010	±0.0014	±11.4	±13.0	±3.5	±0.015	...
01198−0031	A,BC	1000	1686.7	0.540	1.450	123.1	102.8	37.9	...	...
		fixed	±17.4	fixed	±0.021	±9.8	±5.5	±1.1	...	...
01350−2955	A,B	4.5595	2010.127	0.3142	0.1669	168.6	298.9	11.9	0.640	2.92
		±0.0014	±0.006	±0.0022	±0.0006	±6.1	±6.0	±1.7	±0.012	±0.69
01350−2955	AB,C	120.88	1955.24	0.230	1.571	132.5	54.3	36.5	...	...
		±0.83	±0.95	±0.011	±0.018	±3.0	±4.0	±1.2	...	...
02291+6724	Aa,Ab	48.72	1993.21	0.637	0.423	176.6	328.2	148.2	0.322	...
		±0.45	±0.05	±0.004	±0.004	±1.8	±1.9	±1.3	±0.013	...
02291+6724	A,B	2400	940	0.40	6.50	188.0	113.3	102.9	...	...
		fixed	±47	fixed	fixed	±0.9	±3.4	±0.3	...	...
04375+1509	Aa,Ab	2.0097	1999.818	0.405	0.037	319.3	339.2	144.0	0.223	3.85
		±0.0009	±0.011	±0.014	fixed	±11.1	±3.0	fixed	±0.043	±0.06
04375+1509	A,B	124.9	2049.6	0.20	0.667	324.0	260.5	73.3	...	2.23
		±22.6	±12.5	fixed	±0.080	±2.2	±44.3	±1,8	...	±0.23
04397+0952	Aa1,Aa2	1.6732	2013.958	0.426	0.046	286.5	267.7	62.7	0.170	4.47
		±0.0005	±0.013	±0.018	fixed	±10.2	±3.6	±14.3	±0.030	±0.10
04397+0952	Aa,Ab	285	1999.8	0.19	1.637	335.7	253.0	78.6	...	1.91
		fixed	±76	±0.09	±0.136	±4.9	±145	±1.5	...	±0.57
04400+5328	A,B	26.34	1988.98	0.846	0.1727	12.6	42.9	138.4	0.446	...
		±0.05	±0.03	±0.005	±0.0023	±2.5	±2.6	±1.2	±0.009	...
04400+5328	AB,C	660	2011.7	0.405	1.666	286.2	105.1	132.5	...	...
		fixed	±2.7	±0.015	±0.019	±1.8	±5.4	±1.9	...	...
15440+0231	Ba,Bb	6.57	2020.09	0.357	0.189	21.4	230.0	70.4	−0.500	...
		±0.29	±0.08	±0.038	±0.008	±2.7	±9.3	fixed	fixed	...
15440+0231	A,B	900	1936.1	0.435	7.20	54.9	330.9	138.1	...	...
		fixed	±9.9	±0.030	fixed	±7.4	±3.4	±1.5	...	...
16057−0617	Aa,Ab	4.999	2013.16	0.370	0.0521	117.3	8.7	127.0	0.485	...
		±0.005	±0.06	±0.009	±0.0011	±2.5	±5.7	±1.7	±0.053	...
16057−0617	A,B	300	2048.5	0.611	0.877	107.6	141.0	155.0	...	...
		fixed	±4.1	±0.033	±0.009	±24.0	±26.3	fixed	...	...
17066+0039	Ba,Bb	6.311	2013.04	0.400	0.0700	2.4	195.2	29.9	−0.521	...
		±0.031	±0.03	±0.010	±0.0014	±6.2	±7.0	±2.9	±0.031	...
17066+0039	A,B	900	1963.04	0.596	2.264	97.7	356.9	40.0	...	...
		fixed	±1.36	±0.002	±0.023	±3.2	±1.8	fixed	...	...
17157−0949	Ba,Bb	5.257	2011.08	0.46	0.033	52.3	69.0	138.6	−0.436	...
		±0.052	±0.59	±0.11	±0.008	±11.7	±22.5	±24.9	±0.040	...
17157−0949	A,B	137.1	2016.09	0.357	0.344	26.5	280.5	141.4	...	...
		±1.8	±0.26	±0.007	±0.002	±1.2	±1.7	±1.1	...	...
19453−6823	Ba,Bb	4.40	2017.22	0.850	0.0544	148.2	218.9	127.4	−0.344	...
		±0.09	±0.06	fixed	±0.0052	±6.4	±10.3	±7.6	±0.032	...
19453−6823	A,B	84.4	2001.55	0.252	0.475	204.0	336.2	140.0	...	...
		±1.8	±0.86	±0.016	±0.027	±2.6	±1.9	fixed	...	...
22300+0426	Ba,Bb	2.113	2016.60	0.193	0.0412	266.9	151.3	113.1	−0.456	...
		±0.017	±0.06	±0.027	±0.0012	±2.0	±9.0	±1.7	±0.021	
22300+0426	A,B	123.53	2035.38	0.515	0.714	117.1	214.6	89.94	...	...
		±1.26	±0.92	±0.016	±0.009	±0.1	±1.5	±0.04	...	...

TABLE 3
Position measurements and residuals (fragment)

WDS	Syst.	Date (JY)	θ (deg)	ρ ($''$)	σ_ρ ($''$)	(O−C)$_\theta$ (deg)	(O−C)$_\rho$ ($''$)	Ref.[a]
00568+6022	Aa,Ab	1994.7183	161.9	0.0302	0.0020	1.8	0.0009	s
00568+6022	Aa,Ab	1998.7731	98.3	0.0200	0.0020	9.7	0.0032	s
00568+6022	Aa,Ab	1998.7760	69.8	0.0160	0.0020	−19.2	−0.0009	s
00568+6022	Aa,Ab	2000.8744	228.1	0.0250	0.0020	−6.2	−0.0013	s
00568+6022	Aa,Ab	2000.8770	228.9	0.0250	0.0020	−5.5	−0.0013	s
00568+6022	Aa,B	1994.7183	339.7	0.2720	0.0050	−0.2	0.0011	s
00568+6022	Aa,B	1994.7183	339.7	0.2725	0.0050	−0.2	0.0016	s

[a] A: adaptive optics; C: CCD measurement; G: Gaia; H: Hipparcos; J: Finsen's eyeiece micrometer; M: visual micrometer measurement; P: photographic measurement; S: speckle interferometry at SOAR; s: speckle interferometry at other telescopes.

TABLE 4
PARAMETERS OF COMPONENTS OF ADS 784

Parameter	Ab1	Ab2	Aa	B
V (mag)	7.53	8.83	6.57	6.57
$\mathcal{M}$ ($\mathcal{M}_\odot$)	2.44	1.64	3.39	3.39
Spectral type	B9V	A7V	B7V	B7V

from Cole et al. are used to determine the combined orbit of Aa,Ab jointly with the outer orbit of A,B.

The only resolved measurements of Aa,Ab were taken at the 6 m telescope on three epochs, 1994.7, 1998.8, and 2000.9 (I swapped the published quadrant in 2000.9). Micrometric and speckle measurements of the outer pair A,B (without resolving the subsystem) from 1889 to 2010 cover 131 yr or 1.56 outer periods. The photo-center wobble is assumed to be the $f^*/f = 0.32$ fraction of the full wobble to fit the wave in the unresolved measurements. The first speckle-astrometric orbit of the 5-yr pair computed by Cole et al. was based only on the unresolved measurements made before 1990 and had a wobble amplitude of 4 mas.

Differential speckle photometry by Schoeller et al. (1998) in the V band indicates that the magnitudes of Aa and B are similar within 0.1 mag, while Ab is 0.7 mag fainter. The inferred magnitude difference between A and B, 0.45 mag, agrees with its multiple measurements. So, Aa and B have similar luminosities and masses and, together, dominate the combined spectrum. This explains why Cole et al. could not detect the lines of the 5 yr secondary and why they attributed the 4-day binary to B. Using the 50 Myr PARSEC isochrone (Bressan et al. 2012), I found that the magnitude difference between Ab1 and Ab2 of 1.4 mag matches the spectroscopic mass ratio $q_{\rm Ab1,Ab2} = 0.67$. With this assumption, the visual magnitudes of all components are defined (Table 4). Furthermore, I adopt the dynamical parallax of 5.6 mas derived from the A,B orbit and the expected mass sum of $\sim$11 $\mathcal{M}_\odot$. The corresponding spectral types, also listed in Table 4, agree with the spectral classification by Cole et al., except the A7V component Ab2 which they classified as A1V. The two most massive members of this system, B and Aa, have spectral type B7V and are fast rotators.

The adopted parallax of 5.6 mas leads to the inner mass sum of 7.1 $\mathcal{M}_\odot$, in reasonable agreement with 7.5 $\mathcal{M}_\odot$ estimated from the isochrone. The RV amplitude of Ab and its mass, 4.1 $\mathcal{M}_\odot$, correspond to the 3.1 $\mathcal{M}_\odot$ mass for Aa that matches the isochrone mass approximately. Cole et al. noted the large mass of the unseen secondary in the 5-yr subsystem and suggested that it could be a pair of low-mass stars. This hypothesis is no longer viable because speckle interferometry resolved the subsystem Aa,Ab.

The system model in Table 4 implies the mass ratio in the 5-yr subsystem $q_{\rm Aa,Ab} = 1.2$ which, together with the measured light ratio $r = 0.5$, results in the photo-center wobble factor $f^* = 0.20$ and the wobble amplitude of 6.2 mas, similar to the amplitude estimated by Cole et al. However, the calculated wobble factor for the resolved Aa,B positions, $f = 0.55$, disagrees with the measured $f = 0.35 \pm 0.07$. I suspect that the measurement of f based on only three epochs is questionable.

The outer orbit and the estimated masses correspond

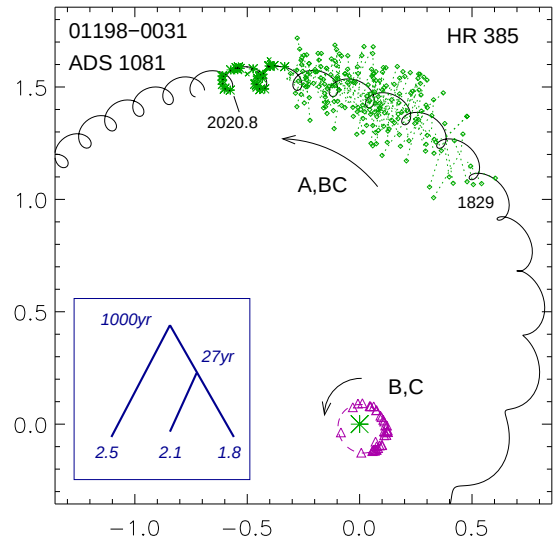

FIG. 2.— Orbits of 42 Cet (ADS 1081), periods 1000 yr and 27 yr.

to the RV amplitudes in the outer orbit of $K_3 = 4.3$ and $K_4 = 9.5$ km s^{-1}. No RV trend associated with the outer orbit is obvious in the RVs measured by Cole et al. Adopting $K_3 = 4.3$ km s^{-1}, I obtain the systemic velocity of -7.6 km s^{-1} or -9.5 km s^{-1}, depending on the node of A,B. The choice of the outer node also defines the mutual inclination. The model proposed here attributes the 4-day subsystem to Ab, hence $\omega_{\rm Ab} = 279\overset{\circ}{.}5$ refers to the secondary component of the 5-yr subsystem. If $\omega_B = 327\overset{\circ}{.}9$ in the outer orbit also refers to the secondary, the mutual inclination between the orbits of A,B and Aa,Ab is $\Phi = 20^\circ \pm 2^\circ$, otherwise the orbits are nearly perpendicular, $\Phi = 90^\circ$. Continued RV monitoring will define the sign of the long-term RV trend and hence the correct node. The inclination of the 4-day subsystem is $i_{\rm Ab1,Ab2} = 63^\circ$.

Relation between ADS 784 and γ Cas (WDS J00567+6043, HD 5394, HR 264), the archetype of Be stars, was noted by Mamajek (2017). The Hipparcos parallax of γ Cas is 5.32±0.56 mas and its RV is -7.4 km s^{-1}; the PMs of these systems also match. Note that γ Cas is a triple system consisting of the 203 day spectroscopic pair, a 60 yr astrometric subsystem, and a faint physical companion at 2.″05. The projected distance between HR 266 and HR 264 is about 1 pc, too large for a bound pair (its orbital period would be $\sim$20 Myr). More likely, these young and massive hierarchical systems are linked together by their common origin.

3.2. *01198−0031 (42 Cet, ADS 1081)*

The bright star HR 385 (42 Cet, ADS 1081) consists of an evolved G8III primary and the tight pair of nearly equal A7V stars B and C (FIN 337 BC). The inner 27 yr orbit is very well defined (Mason et al. 2010), unlike the long-period outer orbit of STF 113 A,BC that lacks coverage despite measurements available since 1829. Gaia gives rather accurate and consistent parallaxes of stars A and BC, and their average, 7.76 mas, defines the distance to the system.

The differential photometry at SOAR gives $\Delta y_{\rm AB} = 0.96 \pm 0.15$ mag, hence the V magnitudes of B and C are 7.50 and 8.46 mag. The orbit of B,C gives a mass sum of

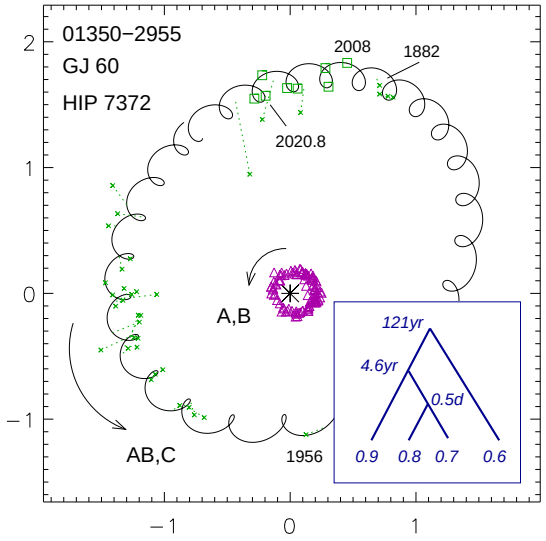

FIG. 3.— Orbits of GJ 60 AB,C (BU 1000, 121 yr) and A,B (DAW 31, 4.56 yr).

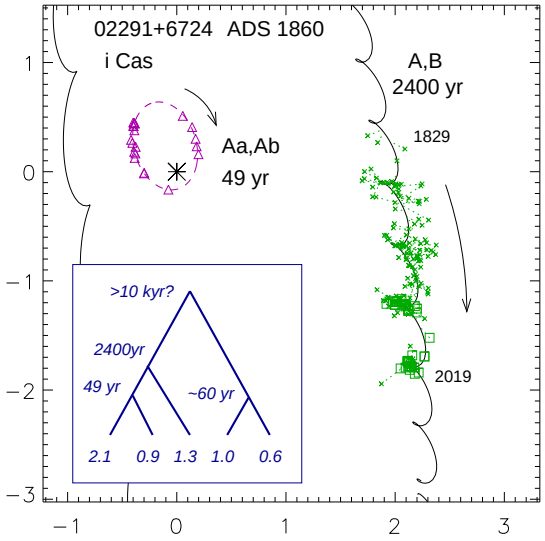

FIG. 4.— Orbits of ι Cas (ADS 1860). A fragment of the outer (2400 yr) orbit and the inner (49 yr) orbit.

3.96 $\mathcal{M}_\odot$. The wobble factor $f = -0.466 \pm 0.016$ implies $q_{\rm BC} = 0.87$, hence the measured masses of B and C are 2.11 and 1.84 $\mathcal{M}_\odot$, somewhat larger than 1.81 and 1.46 $\mathcal{M}_\odot$ estimated from the absolute mangitudes.

The latest outer orbit with $P = 650$ yr (Zirm 2015) yields an unrealistically large outer mass sum of 11.8 $\mathcal{M}_\odot$ vs. 6.5 $\mathcal{M}_\odot$ estimated from the absolute magnitudes. The new outer orbit in Figure 2 has a period arbitrarily fixed at 1000 yr and the fixed eccentricity chosen to obtain the target mass sum. Historic observations that deviated by more than 0.″2 from the orbit were removed from the final fit. A free fit has huge errors, indicating that the data do not really constrain the outer orbit. The tentative outer orbit serves mostly as a reference to measure the wobble factor, and the formal errors of its non-fixed elements are only lower limits. The two mutual inclinations are almost equal, about 40°.

3.3. *01350−2955 (GJ 60)*

The well-studied, solar neighborhood quadruple system GJ 60 consists of four K-type dwarfs with comparable masses (Figure 3). The Gaia parallax of star C, 45.83±0.18 mas, defines the system's distance (the parallax of AB, 38.4 mas, is strongly biased). Star B is an eclipsing binary (designated BB Scl) with a period of 0.4765 day. This bright, nearby, and chromospherically active star is mentioned in 149 references.

This is a rare case where both the outer 121 yr and the inner 4.56 yr visual orbits are well constrained and of good quality. New, slightly updated, orbits are obtained by the full unconstrained fit of 15 elements. Accurate SOAR data from 2008–2020 define the wobble factor $f = 0.640 \pm 0.012$, which clearly shows that B is more massive than A, $q_{\rm A,B} = 1.78$. The inner mass sum is 2.33 $\mathcal{M}_\odot$, hence the measured masses of A and B are 0.84 and 1.49 $\mathcal{M}_\odot$, respectively. The chromospherically active eclipsing subsystem Ba,Bb consists of almost equal mass stars with $q_{\rm Ba,Bb} = 0.97$ (Watson et al. 2001). The estimated mass of C, 0.56 $\mathcal{M}_\odot$, leads to the total system mass of 2.89 $\mathcal{M}_\odot$, which agrees well with 2.75 $\mathcal{M}_\odot$ deduced from the outer orbit and the parallax. If the eclipsing nature of B were not known, the subsystem Ba,Bb could be independently discovered from the excessive mass of B.

The period ratio of the visual pairs is 26.5±0.2. The crude RVs of component A plotted in Figure 5 of Watson et al. (2001) indicate that the node of the 4.6 yr orbit listed here corresponds to the component A. The true node of the outer 121 yr orbit remains unknown, and the small estimated RV amplitude of 1.3 km s^{-1} makes such prospect unlikely. This leaves two options for the mutual inclination, either 28°±2° or 47°. The first choice appears more likely, considering the moderate inner and outer eccentricities (0.31 and 0.23). This hierarchical system resembles other planetary type low-mass hierarchies (Tokovinin 2018b), but its inner eclipsing system is definitely not coplanar with the low-inclination middle and outer orbits. Therefore, the eclipsing subsystem BB Scl should be precessing and this might be detectable by the variable eclipse depth. Analysis of the eclipse time variation can bring additional information on the orbits, but it is outside the scope of this study.

3.4. *02291+6724 (ι Cas, ADS 1860)*

ι Cas (HR 707, ADS 1860) is a well-known quintuple system (Figure 4) with an A5Vp magnetic primary. Three stars A, B, and C were resolved by W. Struve in 1828 (STF 262) at comparable separations and earlier by W. Hershel (his inaccurate measurements are not used here). The 47 yr astrometric subsystem Aa,Ab was detected from the wavy relative motion of A,B (Heintz 1996) and directly resolved for the first time by speckle interferometry in 1982 as CHR 6. In 2002, star C was also resolved into a 0.″4 pair Ca,Cb (CTU 2). The period of Ca,Cb estimated from its separation is ∼60 yr and its orbit is not known yet.

Gaia measured concordant parallaxes of A, B, and C; the latter, most accurate (22.22±0.08 mas), is adopted here. The orbit of A,B with $P = 620$ yr (Heintz 1996), updated here to $P = 2400$ yr, remains essentially unconstrained. Drummond et al. (2003) reached the same conclusion and modeled the observed segment of this orbit by a linear motion. They combined the wobble with direct resolutions of Aa,Ab, computed its first orbit with

$P = 47$ yr, and estimated masses of Aa and Ab; their results are refined here (Figure 4).

The orbit of Aa,Ab is now very well constrained and, together with the Gaia parallax, defines the mass sum of Aa,Ab, 2.91 $\mathcal{M}_\odot$. The wobble factor $f = 0.322 \pm 0.013$ implies the mass ratio of $q_{\rm Aa,Ab} = 0.47$, hence the masses of Aa and Ab are 1.98 and 0.93 $\mathcal{M}_\odot$, respectively. The absolute magnitudes of main-sequence stars Aa and Ab (visual magnitudes 4.65 and 8.63 mag) agree with these masses. The mass of B estimated from its magnitude is 1.28 $\mathcal{M}_\odot$, hence the outer mass sum should be 4.2 $\mathcal{M}_\odot$.

Comparable separations between A, B, and C raise concerns about dynamical stability of this system and thus constrain somewhat the orbit of A,B. On the one hand, its semimajor axis must not be too big compared to the 7″ projected separation between A and C, on the other hand the periastron separation must be at least three times larger than the semimajor axis of Aa,Ab, i.e. >1.″3, which rules out large eccentricities. I fixed the eccentricity of A,B at 0.4 and also fixed the period (2400 yr) and the semimajor axis (6.″5) to values that yield the expected mass sum, 4.2 $\mathcal{M}_\odot$. Without these restrictions, the errors of P, e, a from the free fit are huge. The tentative orbit of A,B proposed by Heintz (1996) has a smaller semimajor axis of 2.″9 and a shorter period and yields the mass sum of 5.9 $\mathcal{M}_\odot$.

The 6.″5 semimajor axis of A,B is in tension with the 7″ projected separation between A and C. A circular orbit of AB,C with $P^* \sim 2$ kyr, estimated from the projected separation, corresponds to the relative orbital speed of $\mu^* = 18$ mas yr^{-1}. I computed the observed speed of the relative motion between AB (center of mass) and C using historic measurements of A,C, subtracting the orbital motion of A, and accounting for the precession in angle. The resulting relative motion speed is only 4.1 mas yr^{-1}. It is directed at an angle of 31° to the vector AB,C (C approaches AB). The slow relative motion is a sign that the actual separation between AB and C in space is substantially larger than the projected separation. In such case, the large semimajor axis of A,B is plausible. However, even if the ratio of the semimajor axes of AB,C and A,B is compatible with the dynamical stability, it is still moderate, suggesting dynamical evolution of this system.

Although the orbit of A,B is poorly constrained, the relative inclination between A,B and Aa,Ab is almost insensitive to the choice of P, e, a and has values of either 46° or 108°. Kozai-Lidov cycles (Naoz 2016) in the inner triple are expected, and the large inner eccentricity of 0.64 may be a manifestation of these cycles.

3.5. *04375+1509 (vB 102)*

This triple system is a G0V star in the Hyades cluster, often referred to as vB 102. It is a single-lined spectroscopic binary with a period of 734.2 day (Griffin 2012) with a faint visual companion discovered in 1989 at 0.″25 separation and designated as CHR 153. Thirty years of interferometric coverage resulted in the first, still tentative visual orbit with $P = 128$ yr (Tokvinin et al. 2019). The Gaia parallax of 20.61±0.46 mas is used here, although it is likely biased by the multiplicity; the PM anomaly is large (Brandt 2018).

The estimated inner semimajor axis is 37 mas, but the inner subsystem remains unresolved owing to the large contrast; however, the wobble in the observed motion of the outer pair is detectable. Two orbits fitted to the speckle measurements and RVs (Figure 5) have a wobble amplitude of 8.5 mas, or $f = 0.22 \pm 0.04$ and $q_{\rm Aa,Ab} = 0.29$ (the inner semimajor axis is computed from the third Kepler's law). The mass of the G0V star Aa is estimated at 1.13 $\mathcal{M}_\odot$, hence the mass of Ab is about 0.32 $\mathcal{M}_\odot$. Most measurements come from SOAR. Griffin (2012) determined the negative linear RV trend caused by the outer system and suggested that $\omega_{\rm A,B}$ is about 270°, as is indeed the case. Note that the RV coverage starts in 1959; it exceeds the speckle coverage and helps to constrain the outer orbit. In the final fit I fixed the outer eccentricity at 0.2 and obtained the expected outer mass sum of 2.16 $\mathcal{M}_\odot$. The outer RV amplitude is 2.23±0.23 km s^{-1} and the system velocity is 41.57 ± 0.41 km s^{-1}.

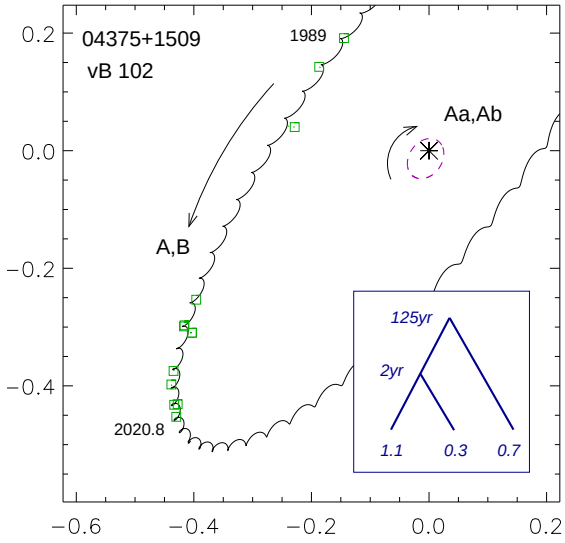

FIG. 5.— Outer orbit of vB 102 (125 yr) with a 2-yr wobble. The inner pair Aa,Ab remains unresolved.

The RV amplitude in the inner orbit is small, 3.85 km s^{-1}, and corresponds to the minimum mass of 0.17 $\mathcal{M}_\odot$ for Ab. Bender & Simon (2008) apparently detected weak lines of Ab in the infrared spectra and deduced the Ab mass of 0.17 $\mathcal{M}_\odot$ from the three RVs, implying a large inclination of the inner orbit. However, their RVs deviate from the orbit more than allowed by the claimed errors (rms 6.6 km s^{-1}), and Griffin considered them as spurious. The wobble amplitude measured here also disagrees with the infrared RVs.

The most unusual result is the apparent counter-rotation in the inner and outer orbits (Figure 5). The free fit gives the inner inclination of $i_{\rm Aa,Ab} = 153° \pm 60°$. I fixed the inclination to 144° for consistency between wobble and RV amplitudes; both correspond to the Ab mass of 0.33 $\mathcal{M}_\odot$. Attempts to fit a co-rotating inner orbit fail. Mutual inclination between the orbits is 72° with fixed inner inclination or 82° ± 47° with the free fit (both nodes are known).

Admittedly, the wobble signal is weak and the astrometric inner orbit is still preliminary. Future Gaia data releases will define this orbit much better if the triple nature of this system can be properly accounted for in the data reduction of this mission.

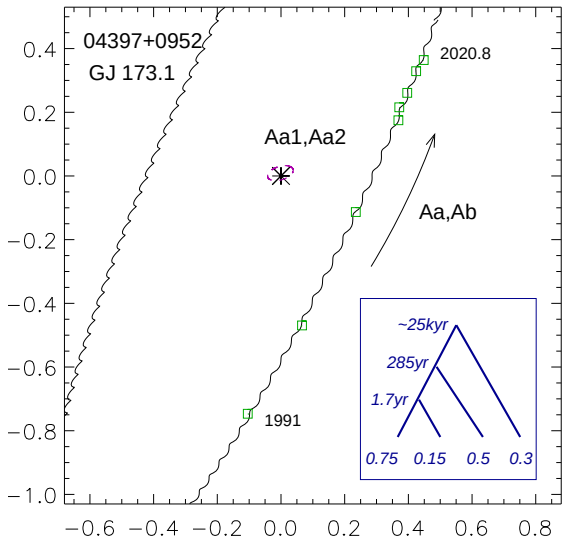

FIG. 6.— Outer orbit of GJ 173.1 Aa,Ab ($P = 285$ yr) with a 1.7 yr wobble.

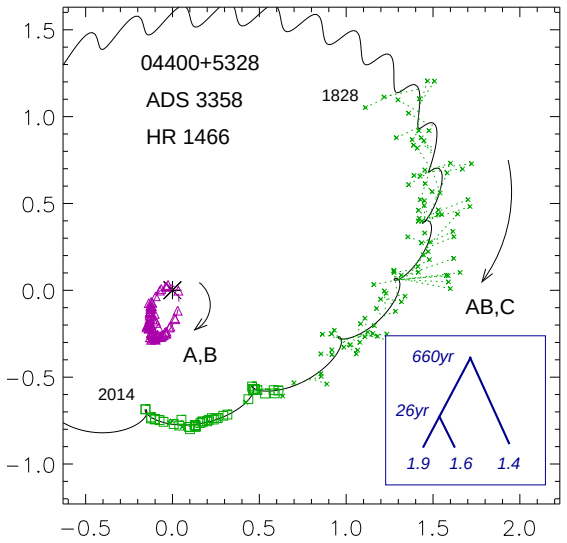

FIG. 7.— Outer (STF 566, 660 yr) and inner (BU 1295, 26 yr) orbits of ADS 3358.

3.6. *04397+0952 (GJ 173.1)*

This nearby (29 pc) quadruple system is composed of low-mass stars (Figure 6). The primary (GJ 173.1, G 83-28) has a spectral type K0V. The 14th magnitude star B (G 83-29) at 34″ has a common PM. The Gaia parallax of B, 34.04±0.12 mas, defines the distance to the system better than the biased parallax of A, 36.80±0.39 mas. Another visual companion Ab, 3.4 mag fainter and at 0.″75 separation, was detected by Hipparcos (HDS 601). Most observations of this pair Aa,Ab come from the speckle program at SOAR. Star Aa is also a single-lined spectroscopic binary Aa1,Aa2 with $P = 610.43$ day (Halbwachs et al. 2018; Sperauskas et al. 2019). The estimated semimajor axis of the innermost orbit, 46 mas, favors detection of the wobble signal.

The orbit of Aa,Ab, including wobble, was fitted to the eight available position measurements of Aa,Ab and 40 published RVs of Aa1 covering the period from 1986 to 2014 (Figure 6). The outer orbit is not fully constrained, and its period is fixed to 285 yr to yield the expected outer mass sum of 1.4 $\mathcal{M}_\odot$; the published preliminary orbit had $P = 204$ yr (Tokovinin 2017a). Even with the fixed period, the errors of some elements are large. A negative RV trend caused by the outer orbit is obvious ($K_3 = 1.9 \pm 0.6$ km s^{-1}), fixing its correct node. The system velocity is $\gamma = -26.2 \pm 1.0$ km s^{-1}.

The wobble factor $f = 0.17 \pm 0.03$ corresponds to $q_{\rm Aa1,Aa2} = 0.20$, so the estimated mass of Aa1, 0.75 $\mathcal{M}_\odot$, leads to the mass of 0.15 $\mathcal{M}_\odot$ for Aa2. The RV amplitude $K_1 = 4.47 \pm 0.10$ km s^{-1} corresponds to the secondary mass of 0.17 $\mathcal{M}_\odot$, hence the two estimates match within errors. The mass of the pair Aa is 0.90 $\mathcal{M}_\odot$, and the outer RV amplitude implies the mass of 0.53 $\mathcal{M}_\odot$ for Ab The absolute magnitude of Ab corresponds to a star of 0.48 $\mathcal{M}_\odot$, in agreement with its spectroscopically estimated mass.

This system resembles the previous one. The orbital nodes are known, and the mutual inclination deduced from the wobble is large, 51°±10°. This result is a consequence of the different node angles Ω, while the inclinations of the inner and outer orbits are similar (both are large). An attempt to force approximate orbit coplanarity fails. The weighted rms residuals of positional measurements are ∼1 mas if the wobble is fitted and 5 mas without wobble.

3.7. *04400+5328 (ADS 3358)*

The classical resolved visual triple system 2 Cam (HR 1466, ADS 3358, spectral type A8V) has been the subject of several studies (e.g. Heintz 1996). Here both orbits are updated using recent speckle measurements (Figure 7). The eccentric orbit of the inner 26 yr pair A,B (BU 1295) is now fully covered by the speckle data and of excellent quality (the weighted rms residuals are 5 mas). Several measurements of the visual magnitude difference in this pair average at $\Delta V_{\rm A,B} = 1.29$ mag. I adopt the masses of 1.94 and 1.45 $\mathcal{M}_\odot$ deduced from the absolute magnitudes of these stars and the dynamical parallax of 13.0 mas. The Gaia parallax of 15.3±0.4 mas is obviously inaccurate and biased (in 2015 the inner pair, unresolved by Gaia, moved rapidly through the periastron at 0.″07 separation) and implies an unrealistically small inner mass sum of 2.1 $\mathcal{M}_\odot$.

The outer orbit of AB,C (STF 566) is not so well defined, despite its numerous measurements available since 1828 that cover a 144° arc. I fixed the outer period to 660 yr and fitted the remaining elements with wobble. The wobble amplitude is very accurate ($f = 0.446 \pm 0.009$) and the measured mass ratio $q_{\rm A,B} = 0.805$ is close to the ratio of the adopted masses, $q_{\rm A,B} = 0.77$. The outer mass sum computed with the dynamical parallax is 4.8 $\mathcal{M}_\odot$, approximately matching the mass of C estimated from its absolute magnitude.

Two possible values of mutual inclination deduced from the orbits are close to each other: 57.°3±2.°2 or 61.°7. Therefore, the orbits are highly inclined. Note the large inner eccentricity of 0.85 suggestive of Kozai-Lidov cycles in this system.

3.8. *15440+0231 (23 Ser, GJ 596.1)*

The bright star 23 Ser (HR 5853, GJ 596.1, ADS 9763), located within 15 pc from the Sun, has been known to host a faint physical satellite B since 1910, when this pair

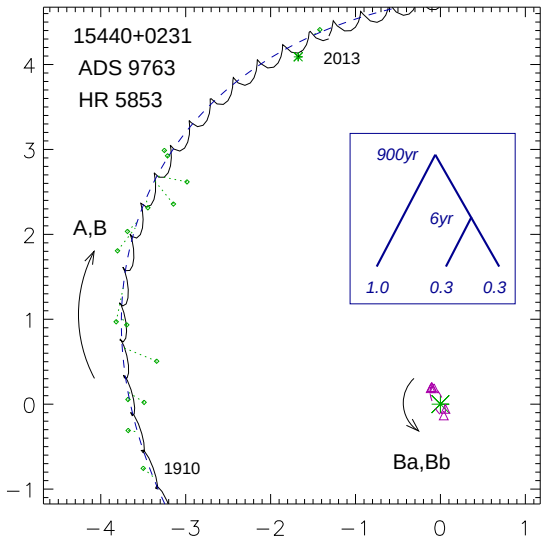

FIG. 8.— Orbits of GJ 596.1 (ADS 9763), periods 900 yr and 6.6 yr.

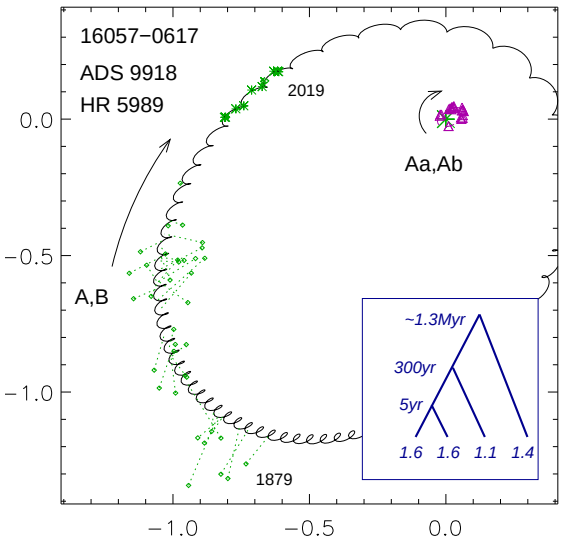

FIG. 9.— Fragment of the the outer orbit (300 yr) of ADS 9918. The inner period of Aa,Ab is 5 yr.

was first measured by R. Aitken (A 2230). The latest orbit of A,B with $P = 529$ yr and $a = 5\farcs04$ computed by Gatewood & Mason (2013) is only preliminary, despite the observed arc of 85°. Other companions mentioned in the WDS are optical. The bright and nearby G3V star A has been studied from various angles, including non-detection of planets.

The M3V star B was resolved into a $0\farcs2$ pair Ba,Bb by Rodriguez et al. (2015) in 2009 and re-discovered at approximately the same position in 2015 by Tokovinin & Horch (2016). They suggested that Ba,Bb has made one full revolution between these observations and its period is about 6 yr. Three additional observations made at SOAR (the last one in 2020.1) now fully constrain this orbit with $P = 6.6$ yr and $a = 0\farcs19$. The Gaia parallax of star A, 67.71±0.07 mas, leads to the inner mass sum of 0.50 $\mathcal{M}_\odot$. The magnitude difference between Ba and Bb measured by Tokovinin & Horch (2016), 0.3 mag, tells us that stars Ba and Bb are similar (a twin), so their masses are 0.26 and 0.24 $\mathcal{M}_\odot$. The photometry by Rodriguez et al. (2015) defines the K magnitude of Ba, 8.08 mag, which corresponds to the mass of 0.27 $\mathcal{M}_\odot$ according to the standard relations.

The estimated mass of A, 0.98 $\mathcal{M}_\odot$, implies the outer mass sum of 1.48 $\mathcal{M}_\odot$. I fixed the outer elements $P = 900$ yr and $a = 7\farcs2$ to match this mass sum and fitted the remaining elements (Figure 8). The orbital motion changes the PM of A. According to Brandt (2018), the Gaia PM anomaly of star A is $(+1.3, +3.8)$ mas yr^{-1}. The difference between the orbital speed of B in 2015.5 and its mean speed between 1991.25 and 2015.5 is $(-3.1, -7.2)$ mas yr^{-1}, in qualitative agreement with the PM anomaly. The RV amplitude in the outer orbit is ∼1 km s^{-1}, explaining the linear RV trend of −3.04 m s^{-1} per year detected by Butler et al. (2017).

Only one resolved measurement of A,Ba is available, hence the wobble amplitude remains unknown; I fixed it to $f = -0.5$. Opposite rotation directions in the inner and outer pairs are evident. The relative inclinations are 75°±3° or 141°. This triple system is definitely not co-planar.

3.9. *16057−0617 (ADS 9918)*

This is a classical visual triple system (ADS 9918, HR 5989) with two known orbits and the fourth distant (260″) and bright component E (HIP 78822, HD 144309) with common PM and parallax. The Gaia parallax of E, 12.03±0.05 mas, defines the distance better than the less accurate and potentially biased parallax of A, 12.2±0.3 mas.

The outer pair A,B (BU 948), discovered in 1879 at $1\farcs5$ separation, is slowly closing down; the observed arc is 75° (Figure 9). The inner subsystem Aa,Ab discovered by W. Finsen in 1964 (FIN 384) has an orbital period of exactly 5 yr. Components Aa and Ab are equal and their separation never exceeds 70 mas. The orbit of Aa,Ab has a good coverage by speckle interferometry. Measurements of Aa,Ab at close separations in 2008 at SOAR and in 2017 at Gemini (Horch et al. 2019), at phases not covered before, further constrain the orbit. The inner mass sum of 3.26 $\mathcal{M}_\odot$ matches the absolute magnitude of its equal components of spectral type F2IV.

The outer orbit with $P = 459$ yr and $e = 0.65$ was computed by Zirm (2014). The data do not constrain the period, so I fixed it to 300 yr and, furthermore, fixed the outer inclination to 155° to obtain the expected outer mass sum, 4.3 $\mathcal{M}_\odot$ (the free fit gives $i_{AB} = 158° \pm 11°$). The wobble factor $f = 0.49 \pm 0.05$ confirms that the masses of Aa and Ab are equal. However, these stars were sometimes swapped and some outer measurements referred to Ab,B instead of Aa,B; these cases are rectified here. Moreover, the measurement of Aa,B at Gemini in 2017.4 revealed inaccurate calibration of the scale and was given a low weight, while the tight inner pair Aa,Ab was measured well at 27.5 mas separation. The mutual inclination between the orbits is 32° or 78°; the smaller inclination appears more likely.

3.10. *17066+0039 (ADS 10341)*

The outer pair of ADS 10341 (BU 823) is known since 1881. The latest visual orbit of A,B with $P = 532$ yr computed by Hartkopf & Mason (2000) is still preliminary, although the observed arc slightly exceeds 180°(Figure 10).

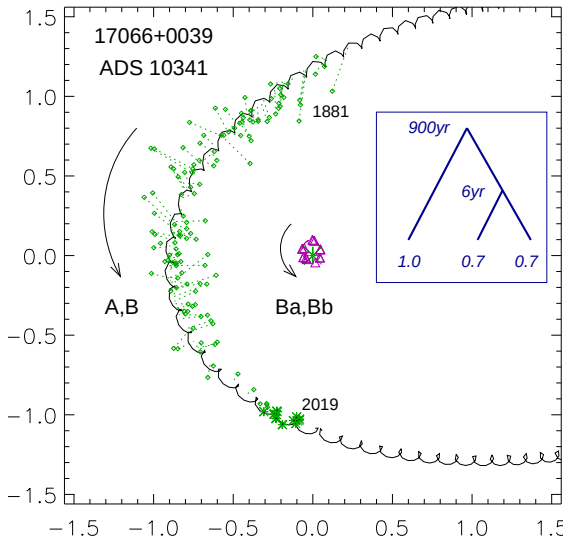

FIG. 10.— The outer orbit (900 yr) with wobble and the inner 6.3 yr orbit of ADS 10341.

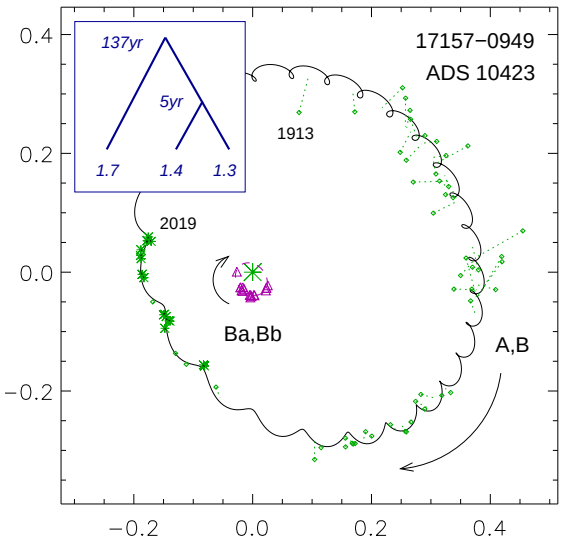

FIG. 11.— Orbits of ADS 10423 (137 yr and 5.26 yr).

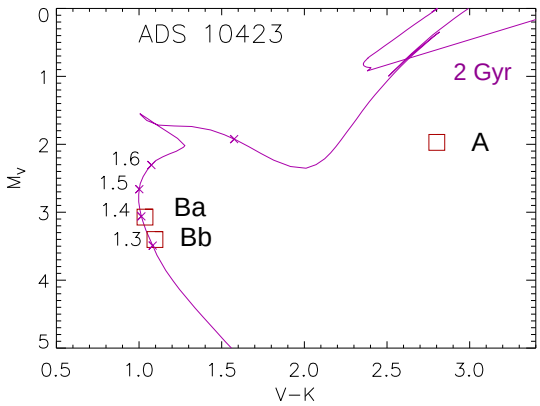

FIG. 12.— Components of ADS 10423 in the $V, V-K$ CMD (squares) and the 2 Gyr isochrone for solar metallicity (Bressan et al. 2012). Numbers and crosses mark masses from 1.3 to 1.7 $\mathcal{M}_\odot$ on the isochrone.

The main G0V star A has an estimated mass of 0.98 $\mathcal{M}_\odot$ and its Gaia parallax is 17.90±0.07 mas.

The secondary component B was resolved at SOAR in 2009 into a close pair Ba,Bb (TOK 52). The orbit of Ba,Bb with $P = 6.3$ yr is well constrained (Tokovinin 2016). It is slightly updated here using the latest measurements (e.g. Horch et al. 2019). The mass sum of Ba,Bb, 1.50 $\mathcal{M}_\odot$, agrees with masses estimated from the absolute magnitudes of Ba and Bb. The magnitude difference between Ba and Bb is small, ∼0.1 mag, and the wobble factor $f = -0.52 \pm 0.03$ confirms the equality of masses. No wobble is therefore expected in the positions of A,B, and only the resolved measurements of A,Ba at SOAR show characteristic loops with a 6 yr period.

The period of A,B is between 350 yr and 1000 yr. The curvature of the observed arc constrains the mass sum to values between 2 and 2.5 $\mathcal{M}_\odot$. The period in the free fit has a large error, hence it can be selected within the error range. Orbits with shorter periods have smaller eccentricities and inclinations and the mass sum around 2 $\mathcal{M}_\odot$. I fix $P_{A,B} = 900$ yr and $i_{A,B} = 40°$ to obtain the mass sum of 2.5 $\mathcal{M}_\odot$, in agreement with the estimated mass of A.

The two possible values of mutual inclination, 60° or 46°, are similar. If a shorter outer period is enforced, the mutual inclination is reduced to ∼33°. The inner and outer orbits are thus aligned, but only approximately so.

3.11. *17157−0949 (ADS 10423)*

The 7th mag star HD 156034 was resolved by R. Aitken in 1913 as a 0.″3 pair with components of similar brightness (ADS 10423, A 2592). Its orbit has been calculated and re-calculated many times. Now most of the outer orbit with $P = 137$ yr is covered and its elements are quite accurate (Figure 11).

The inner subsystem Ba,Bb (TOK 53) was discovered at SOAR in 2009. Its preliminary 5 yr orbit (Tokovinin et al. 2015b) is well defined now, after two complete revolutions have been monitored at SOAR. The weighted rms residuals of Ba,Bb positions are 1.5 mas. The latest measurement of Ba,Bb made in 2020.2 at 27 mas separation (below the diffraction limit) has a large residual in angle and is assigned a low weight. The inner semimajor axis is 33 mas and the Ba,Bb pair is not resolved at SOAR near periastron. The wobble amplitude is 14.5 mas ($f = -0.44 \pm 0.04$).

This triple system is lucky in having both orbits well constrained, but its analysis is nevertheless tricky because the distance is not accurately measured and the components are evolved. The original and revised Hipparcos parallaxes are 5.7±1.3 mas and 4.9±0.9 mas, respectively. Gaia normally does not measure parallaxes and PMs of close binaries (A,B was at 0.″18 in 2015.5), but it did so for ADS 10423; the Gaia parallax of 2.8±0.9 mas is obviously erroneous. All three quoted trigonometric parallaxes correspond to unrealistically large masses. I adopt the dynamical parallax of 7.9 mas based on the orbits and estimated masses.

The spectral type F5V quoted in Simbad disagrees strongly with the combined color $V - K = 2.40$ mag that corresponds to the spectral type K3, matching the low effective temperature of 4933 K estimated by Gaia. This contradiction suggests that star A is redder and more evolved compared to the less massive stars Ba and Bb. The light of B dominates at short wavelengths and

its estimated spectral type is indeed F5V. I propose the system model where star A has a mass of 1.705 $\mathcal{M}_\odot$ and stars Ba and Bb have masses of 1.38 and 1.30 $\mathcal{M}_\odot$, respectively. The age of the system is about 2 Gyr.

Figure 12 compares absolute magnitudes and colors of the components with the 2 Gyr PARSEC isochrone for solar metallicity (Bressan et al. 2012). However, the $V-K$ colors of stars are guessed rather than measured because no differential photometry in the K band is available. I use the magnitude difference between Ba and Bb of 0.32 and 0.30 mag measured by Horch et al. (2019) at wavelengths of 692 nm and 880 nm (roughly in the R and I bands) and confirmed independently by the differential speckle photometry at SOAR, e.g. $\Delta y_{\rm Ba,Bb} = 0.33$ mag. According to Horch et al. (2019), the magnitude difference between A and Ba is 1.30 and 1.66 mag in the R and I bands, and SOAR complements this with $\Delta y_{\rm A,Ba} = 1.11$ mag. Photometry confirms that Ba is bluer than A. The two-color photometry of A and B provided by Tycho is discrepant and I ignore it, while the Hipparcos measurement $\Delta Hp_{\rm A,B} = 0.27$ mag appears reliable. The V magnitudes of A, Ba, and Bb deduced from the combined and differential photometry are 7.51, 8.61, and 8.94 mag, respectively. I assign the K magnitudes of Ba and Bb to match their positions on the isochrone (and the spectral type F5), and obtain the K magnitude of A from the combined photometry; the result is 4.71, 7.57, and 7.85 mag.

The proposed system model defines the masses of the components quoted above and matches the differential photometry in the V and I bands. The outer mass sum of 4.4 $\mathcal{M}_\odot$ deduced from the model and the outer orbit correspond to the dynamical parallax of 7.9 mas. With this parallax, the less accurate inner orbit gives the mass sum of 2.6 $\mathcal{M}_\odot$ for Ba,Bb, in good agreement with the model. The model thus matches both the orbits and the photometry. The inner mass ratio $q_{\rm Ba,Bb} = 0.93$ corresponds to $f = 0.48$, which agrees, within errors, with the measured wobble factor $f = 0.44$. If additional multicolor photometry and high-resolution spectroscopy are secured in the future and properly interpreted, this system might offer a valuable test of the isochrones because Aa is just leaving the main sequence.

Mutual inclination between the orbits is either $29°\pm14°$or $77°$; the first, smallest value seems more likely. It is worth mentioning that the RV of this star (apparently dominated by the late-type spectrum of A) has been monitored by Tokovinin & Smekhov (2002) and found to be constant.

3.12. *19453−6823 (HIP 97196)*

An inconspicuous 10th magnitude K-type dwarf star HIP 97196 has been resolved by Hipparcos into a $0\farcs3$ pair (HDS 2806) with unequal components, $\Delta Hp = 2.63$ mag. The binary has been observed for the second time at SOAR in 2014.3, and its secondary component was resolved into a $0\farcs05$ pair Ba,Bb (TOK 425) with $\Delta I = 1.2$ mag. As expected, the inner pair is a fast mover, and its first orbit with $P = 4.1$ yr was published by Tokvinin et al. (2019). The insert in Figure 13 shows a typical speckle auto-correlation function (ACF) to illustrate the difficulty of measuring this tight and faint triple system with substantial contrast. All observations at SOAR were made in the I filter, the last one in 2020.8.

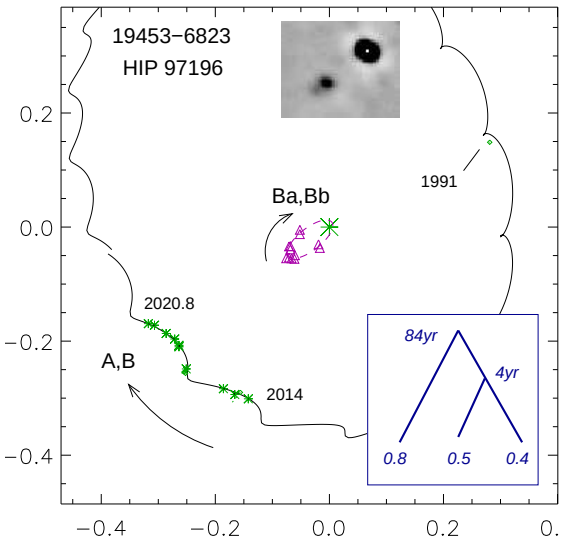

FIG. 13.— Orbits of HIP 97196 (84 and 4.4 yr). The insert shows the speckle ACF recorded in 2018.8.

About half of the outer orbit is now covered, and the first set of its elements is computed here. However, the coverage is uneven, with a large gap between 1991 and 2014. The orbit is not fully constrained: shorter periods with smaller eccentricity also fit the data. I fixed the outer inclination to 140° to match the expected mass sum. The eccentric ($e_{\rm Ba,Bb} = 0.85$) inner orbit is also not very accurate because its part near the periastron is below the resolution limit. The quadrants of Ba,Bb are defined, so the alternative low-eccentricity orbit with double period is not allowed. The closest resolved measurement of Ba,Bb at 36 mas separation was made in 2017.4 at Gemini (Horch et al. 2019), at 880 nm wavelength. Their simultaneous measurement at 692 nm has discordant photometry and is given a low weight, so this object is a difficult one even for an 8 m telescope.

The Gaia parallax of 21.02 ± 0.39 mas is not very accurate and possibly biased, although it agrees with the revised Hipparcos parallax of 21.3 ± 1.9 mas (van Leeuwen 2007). I adopt the Gaia parallax and estimate masses from the standard relations and absolute I magnitudes. The combined $I = 8.83$ mag is deduced by interpolation from other bands (no direct measurement of I is found in the literature), and I adopt $\Delta I_{\rm A,B} = 2.0$ mag and $\Delta I_{\rm Ba,Bb} = 1.2$ mag. The estimated masses of A, Ba, and Bb are 0.78, 0.54, and 0.40 $\mathcal{M}_\odot$, respectively. Main-sequence stars with these masses match the combined magnitudes in the V and K bands and the magnitude differences, the orbits, and the Gaia parallax. The model implies an inner mass ratio of $q_{\rm Ba,Bb} = 0.74$ and $f = -0.43$, while the measured wobble factor is $f = -0.34 \pm 0.03$.

The outer orbit matches the PM anomaly of $(17.8, 7.6)$ mas yr^{-1} in 1991.25 determined by Brandt (2018) because the corresponding orbital motion of B relative to A, $(-31.3, -20.5)$ mas yr^{-1}, has approximately opposite direction and is two times faster. The photo-center wobble factor f^* in the outer orbit in the V band, computed using the adopted masses, is 0.47. The Gaia PM anomaly, $(-1.2, -19.2)$ mas yr^{-1}, does not agree so well with the orbital motion of AB, $(9.3, 37.73)$ mas yr^{-1}, possibly because of the shorter time span of Gaia data

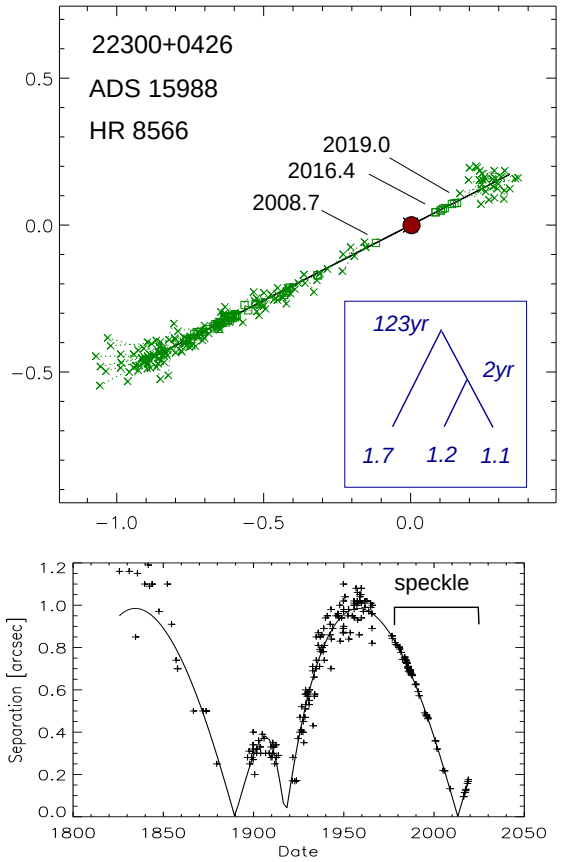

FIG. 14.— Visual orbit of the outer subsystem in ADS 15988 (STF 2192). Top: orbit on the sky, bottom: separation vs. time.

and the larger effect of the inner subsystem on the photocenter motion in the G band. Astrometric signal caused by both orbits should be recovered correctly in the future Gaia data releases that will also yield the unbiased parallax.

Both inner and outer subsystems of HIP 97196 rotate clockwise, but the relative inclination is substantial, $\Phi = 42° \pm 7°$ or $\Phi = 80°$; the period ratio is about 20. The current linear apparent configuration of these stars on the sky suggests coplanar and highly inclined orbits, but this impression is misleading. It is likely that this triple system goes through Kozai-Lidov cycles and currently is in the low-inclination and high-e phase of the cycle. Evidently, this hierarchical system differs from the quasi-coplanar "dancing twins" with comparably small masses and short periods (Tokovinin 2018b) in several important respects: large mutual inclination, large inner eccentricity, and unequal masses of the components.

The spatial velocity of this system $U, V, W = (45, 4, -46)$ km s^{-1} strongly suggests that it is old and possibly metal-poor. Its further detailed study will be interesting for various reasons, e.g. to measure accurate masses and luminosities and to probe the long-term dynamical evolution. Continued speckle monitoring, relative photometry in the infra-red, and high-resolution spectroscopy are needed.

3.13. *22300+0426 (ADS 15988)*

The bright star 37 Peg (HR 8566, ADS 15988) was resolved as a 1″ visual pair by W. Struve in 1825 and is known as STF 2192. This pair slowly closed down during the 19th century, went through the periastron around 1911, opened up again and started to close down in the 2nd half of the 20th century. From 1976 on, accurate speckle interferometry replaced visual micrometer measurements, providing excellent coverage of the decreasing angular separation. This bright pair was frequently observed by speckle interferometry, possibly as a convenient calibrator. Its latest orbit by Söderhjelm (1999) has a grade 2, i.e. is reliable and accurate by current standards. The inclination is 90°, so the orbit is based only on the measured separations (Figure 14). The WDS database contains 335 measurements of its relative position.

The parallax of 37 Peg was measured by Hipparcos at 18.93±1.23 mas, revised to 19.1 mas by Söderhjelm (1999) and to 19.58±0.58 by van Leeuwen (2007). The Gaia parallax of 18.84±0.39 (53 pc distance) is only slightly more accurate, possibly because this star is bright and its astrometry is disturbed by the orbital acceleration. Fortunately, motion in the outer orbit between 1991 and 2015 was almost linear and the PM anomaly is small (Brandt 2018). All parallax measurements are mutually consistent, within their errors. The orbital elements and the masses estimated here favor a slightly smaller dynamical parallax of 18.4 mas.

This $V = 5.5$ mag star attracted attention of observers for various reasons. It was monitored spectroscopically by Abt & Levy (1976) in a survey of bright solar-type stars. They found a spectroscopic subsystem with a period of 372.4 day and a semi-amplitude of 8.2 km s^{-1}. However, this orbit, together with other orbits from that paper, has not been confirmed by subsequent observations. The star is no longer listed as a spectroscopic binary in the current catalog. And yet it is triple!

ADS 15988 was observed by speckle interferometry at SOAR for the first time in 2008.7 when it still approached the conjunction. Shortly after the conjunction, in 2015, the pair was re-visited at SOAR twice. On the second visit in 2015.9, star B was clearly resolved into a close 46 mas subsystem (Figure 15) with nearly equal components Ba and Bb (Tokovinin et al. 2016). We can only guess why the subsystem Ba,Bb has not been noted much earlier in numerous speckle observations with 4 m telescopes. Maybe the fact that it is such a well-known binary prevented observers from noting that the secondary component is itself a close pair.

The small separation of Ba,Bb implied a short orbital period. For this reason, the object was frequently observed at SOAR. The subsystem played "hide and seek": it disappeared in 2016 but was resolved again in 2017–2020. In 2017, the subsystem was also measured with the 8 m Gemini telescope (Horch et al. 2019). Finally, the measurements accumulated to date allow calculation of the orbit of Ba,Bb with a period of 2.1 yr (Figure 15). The orbit of Ba,Bb successfully models the measurements (the weighted rms residuals are 0.9 mas) and predicts small separations for the dates when the subsystem was not resolved, e.g. in 2008.7. The observations cover two orbital periods of Ba,Bb. The Gaia parallax of 18.84±0.39 mas corresponds to the inner mass sum of 2.34±0.25 $\mathcal{M}_\odot$.

The edge-on orbit of A,B (Figure 14) computed by Söderhjelm (1999) fits the latest measurements rather well and, in principle, does not require revision. How-

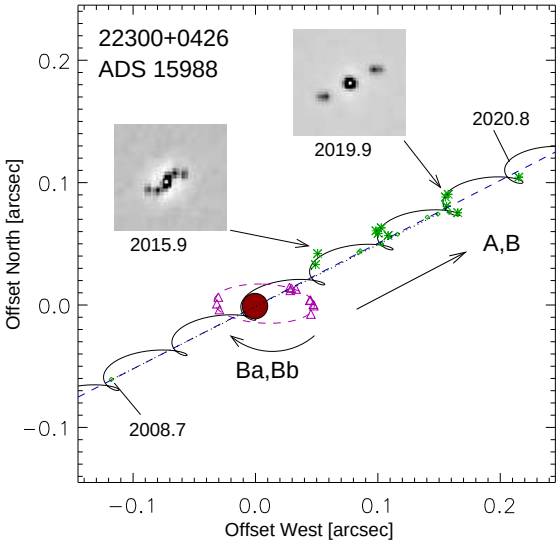

FIG. 15.— Fragment of the outer orbit of ADS 15988 covered at SOAR. The wavy line is the position of Ba relative to A (the red circle at the coordinate origin) affected by the wobble, asterisks show the measured positions of Ba. Small crosses and the blue dash line show the unresolved measurements of B without wobble. The inner orbit is over-plotted on the same scale (the magenta ellipse and triangles).

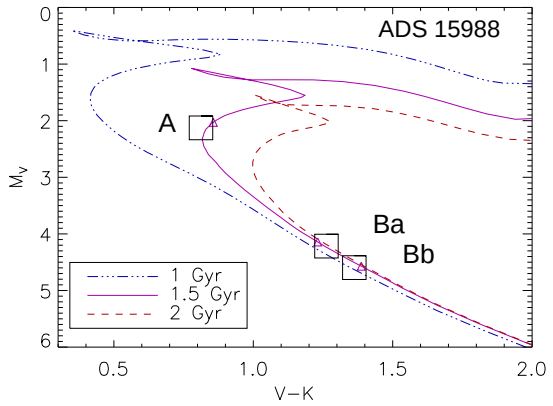

FIG. 16.— Location of the components of ADS 15988 (squares) on the color-magnitude diagram. The lines are PARSEC isochrones (Bressan et al. 2012) for solar metallicity. Small triangles mark the masses of 1.70, 1.17, and 1.10 $\mathcal{M}_\odot$ on the 1.5-Gyr isochrone.

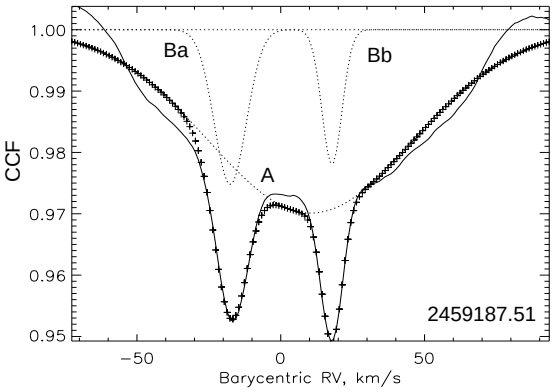

FIG. 17.— Cross-correlation function (line) of the spectrum of ADS 15988 taken on 2020 December 3 showing its triple-lined nature. The dotted curves are fitted Gaussians and the crosses are their sum. The RVs of Ba, Bb, and A are −17.56, 17.81, and 10.50 km s^{-1}, respectively.

TABLE 5
PARAMETERS OF COMPONENTS OF ADS 15988

Parameter	AB	A	Ba	Bb
V (mag)	5.51	5.75	7.84	8.22
$V-K$ (mag)	0.93	0.81:	1.26:	1.36:
$\mathcal{M}$ ($\mathcal{M}_\odot$)	3.97	1.70	1.17	1.10

ever, the errors of orbital elements are not given in the above paper, and the system of weights is not known. Here the orbit is re-fitted using all available data with appropriate weights and rejecting the outliers. The orbit of A,B serves as a reference for determination of the inner mass ratio from the resolved measurements of the subsystem. Both orbits were fitted simultaneously by `orbit4.pro` using only speckle measurements and fixing all outer elements except T_0, Ω, and i to the values determined from the historic data set. The result (Figure 15) yields the wobble factor $f = 0.46 \pm 0.02$, hence $q_{\rm Ba,Bb} = 0.83 \pm 0.07$.

Table 5 gives the combined and individual magnitudes of ADS 15988 in the V and K bands based on the available data. The magnitude difference between A and B has been measured by Davidson et al. (2009) ($\Delta V = 1.50\pm0.05$ mag, $\Delta R = 1.35\pm0.07$ mag), by Fabricius & Makarov (2000) ($\Delta V = 1.51$ mag, $\Delta B = 1.78$ mag), and by Hipparcos ($\Delta Hp = 1.539$ mag). It is clear that B is slightly redder than A. The mean of six measurements of the magnitude difference between Ba and Bb at SOAR in the y band (close to V) is 0.38 mag, with an rms scatter of 0.05 mag. The differential photometry and the combined $V_{\rm AB} = 5.51$ mag define the components' individual magnitudes. However, no differential photometry in the K band is available, and only the combined $V-K$ color is known. This leaves two unknowns for the three $V-K$ colors of the components. The colors of Ba and Bb in Table 5 are chosen to place them on the main sequence in the CMD (Figure 16), thus also defining the color of A. Obviously, this is only a plausible guess, not a real measurement.

The most massive star A in this system appears to be slightly evolved off the main sequence; it is located on the 1.5 Gyr isochrone. The masses of the stars derived from this isochrone and the absolute V magnitudes are listed in the last line of Table 5. Adopting these masses, the magnitudes in other photometric bands can be deduced from the isochrone. These estimates lead to the magnitude difference between A and B of 1.74 and 1.38 mag in the B and R bands, respectively, in agreement with the observed differential colors.

The masses of Ba and Bb estimated from the isochrone correspond to the mass sum of 2.27 $\mathcal{M}_\odot$ which agrees with the measured mass sum of 2.34±0.25, within the error. The isochrone masses imply the inner mass ratio of 0.94, somewhat larger than 0.83±0.07 derived from the wobble amplitude. The total mass sum deduced from the isochrone, 3.97 $\mathcal{M}_\odot$, is slightly larger than measured (3.56±0.28 $\mathcal{M}_\odot$) and corresponds to the dynamical parallax of 18.4 mas.

A high-resolution spectrum taken on 2020 December 3 (Figure 17) shows lines of all three components. The RVs match qualitatively their expected values and allow correct identification of the orbital nodes. They are not

used in the orbital fit, pending additional observations. Future joint analysis of RVs and resolved measurements will allow us to measure masses without relying on the isochrone and parallax.

The mutual inclination is $37.^{\circ}5 \pm 2.^{\circ}0$. Inclination of the outer orbit, $89.^{\circ}9 \pm 0.^{\circ}06$, suggests possible eclipses during the conjunctions. However, star B is a close pair, so only eclipses involving its components can take place. The next conjunction will happen around 2042.

4. SUMMARY

In most hierarchical systems studied here the outer binaries are bright classical pairs with ADS numbers (Aitken 1932) observed for a century or longer. Their inner subsystems are either discovered recently or also known from the era of visual observations. The published orbital elements are revised here using recent observations and appropriate weights and accounting for the wobble. Some long-period orbits remain poorly constrained even when the expected mass sum is used as additional input. Joint fitting of the inner and outer orbits using all available information is the main result of this paper. The orbits, together with the estimated masses, will enable detailed study of the internal dynamics in these systems (e.g. Xia & Fu 2015; Hamers 2020). The ratios of inner and outer separations are moderate, so some interaction between the orbits is expected.

Our small and random sample of hierarchical systems is not statistically relevant, but it does illustrate the diversity of their architectures, ranging from approximately aligned configurations with small eccentricities to highly inclined or even counter-rotating systems where eccentric inner orbits likely result from the Kozai-Lidov cycles. This study enlarges the small collection of systems with resolved inner and outer orbits. Previous analysis of such systems (Tokovinin 2017b) indicated that a mixture of hierarchies aligned within 70° and those with uncorrelated orbits, in a 8:2 proportion, matches the observed distribution of mutual inclinations Φ.

Some data used here were obtained at the Southern Astrophysical Research (SOAR) telescope. This work used the SIMBAD service operated by Centre des Données Stellaires (Strasbourg, France), bibliographic references from the Astrophysics Data System maintained by SAO/NASA, and the Washington Double Star Catalog maintained at USNO; I thank B. Mason for extracting historic measurements from the WDS database. This work has made use of data from the European Space Agency (ESA) mission Gaia (https://www.cosmos.esa.int/gaia), processed by the Gaia Data Processing and Analysis Consortium (DPAC, https://www.cosmos.esa.int/web/gaia/dpac/consortium). Funding for the DPAC has been provided by national institutions, in particular the institutions participating in the Gaia Multilateral Agreement. Work of the author is funded by the NSF's NOIRLab.

REFERENCES

Abt, H. & Levy, S. 1976, ApJS, 30, 273
Aitken, R. G. 1932. New General Catalogue of Double Stars within 120° of the North Pole. Carnegie Inst. Washington D.C. Publ. 417
Balega, I. I., Balega, Yu. Yu., Hofmann, K.-H., et al. 1999, AstL, 25, 797
Bender, C. F. & Simon, M. 2008, ApJ, 689, 4168
Brandt, T. D. 2018, ApJS, 239, 31
Bressan, A., Marigo, P., Girardi, L., et al. 2012, MNRAS, 427, 127
Butler, R. P., Vogt, S. S., Laughlin, G., et al. 2017, AJ, 153, 208
Cole, W. A., Fekel, F. C., & Hartkopf, W. I. 1992, AJ, 103, 1357
Davidson, J. W., Baptista, B. J., Horch, E. P., et al. 2009, AJ, 138, 1354
Docobo, J. A. & Andrade, M. 2006, ApJ, 652, 681
Drummond, J., Milster, S., Ryan, P., et al. 2003, ApJ, 585, 1007
Fabricius, C. & Makarov, V. V. 2000, A&A, 356, 141
Gaia Collaboration, Brown, A. G. A., Vallenari, A., Prusti, T., et al. 2018, A&A, 595, 2 (Vizier Catalog I/345/gaia2).
Gatewood, G. & Mason, B. D. 2013, Inf. Circ. 181, 1
Griffin, R. F. 2012, ApA, 33, 296
Halbwachs, J. -L., Mayor, M., & Udry, S. 2018, A&A, 619A, 81
Hamers, A. 2020, MNRAS, 494, 5298
Hartkopf, W. I. & Mason, B. D. 2000, Inf. Circ. 142, 1
Hartkopf, W. I., Mason, B. D. & Worley, C. E. 2001, AJ, 122, 3472
Heintz, W. D. 1996, AJ, 111, 408
Horch, E. P., Tokovinin, A., Weiss, S. A., et al. 2019, AJ, 157, 56
Mamajek, E. 2017, JDSO, 13, 264
Mason, B. D., Hartkopf, W. I., & Tokovinin, A. 2010, AJ, 140, 735
Mason, B. D., Wycoff, G. L., Hartkopf, W. I., Douglass, G. G. & Worley, C. E. 2001, AJ, 122, 3466 (WDS)
Naoz, S. 2016, ARAA, 54, 441
Pecaut, M. J. & Mamajek, E. E. 2013, ApJS, 208, 9
Penoyre, Z., Belokurov, V., & Wyn, E. N. 2020, MNRAS, 495, 321

Facility: SOAR

Rodriguez, D. R., Duchêne, G., Tom, H., et al. 2015, MNRAS, 449, 3160
Schoeller, M., Balega, I. I., Balega, Y. Y., et al. 1998, AstL, 24,283
Söderhjelm, S. 1999, A&A, 341, 121
Sperauskas, J., Deveikis, V., & Tokovinin, A. 2019, A&A, 626A, 31
Tokovinin, A. 2016, AJ, 152, 138
Tokovinin, A. 2017a, Inf. Circ. 193, 1
Tokovinin, A. 2017b, ApJ, 844, 103
Tokovinin, A. 2018a, ApJS, 235, 6
Tokovinin, A. 2018b, AJ, 156, 160
Tokovinin, A. & Horch, E. 2016, AJ, 152, 116
Tokovinin, A., Latham, D. W. & Mason, B. D. 2015a, AJ, 149, 195
Tokovinin, A. & Latham, D. W. 2017, ApJ, 838, 54
Tokovinin, A. & Latham, D. W. 2020, AJ, 160, 251
Tokovinin, A., Mason, B. D., Mendez, R. A., et al., 2015b, AJ, 150, 50
Tokovinin, A., Mason, B. D., Hartkopf, W. I., et al., 2016, AJ, 151, 153
Tokovinin, A., Mason, B. D., Hartkopf, W. I., et al. 2018, AJ, 155, 235
Tokovinin, A., Mason, B.D., Mendez, R. A., et al., 2019, AJ, 158, 48
Tokovinin, A., Mason, B. D., Mendez, R. A., et al. 2020, AJ, 160, 7
Tokovinin, A. A. & Smekhov, M. G. 2002, A&A, 383, 118
van Leeuwen, F. 2007, A&A, 474, 653
Watson, L. C., Pritchard, J. D., Hearnshaw, J. B., et al. 2001, MNRAS, 325, 143
Xia, F. & Fu, Y. 2015, ApJ, 814, 64
Zirm, H. 2014, Inf. Circ. 182, 1
Zirm, H. 2015, Inf. Circ. 185, 1